

Article

Experimental Performance Analysis of Hardware-Based Link Quality Estimation Modelling Applied to Smart Grid Communications

Natthanan Tangsunantham and Chaiyod Pirak *

Research Centre of Advanced Metering Infrastructure (AMI), The Sirindhorn International Thai-German Graduate School of Engineering (TGGS), King Mongkut's University of Technology North Bangkok, 1518 Pracharat 1 Rd. Bangsue, Bangkok 10800, Thailand; s5909101960515@email.kmutnb.ac.th

* Correspondence: chaiyod.p@tggs.kmutnb.ac.th

Abstract: The smart grid is the modern electricity grid, which significantly improves the efficiency, reliability, and sustainability of electricity transmission systems. The advanced metering infrastructure (AMI) system, which is the essential system in the smart grid, enables real-time data collection and data analysis obtained from smart meters (SMs) and other devices through last-mile communication networks. In this paper, the hardware-based link quality estimation (LQE) was modeled, namely an SNR-based model, a mapping model, and an RSSI- and PRR-based logistic regression model, and their performance was then evaluated by the root mean-squared error (RMSE) with the empirical data. The SNR-based and mapping models were formulated by the packet error probability, whereas the RSSI- and PRR-based logistic regression model was formulated by the empirical data fitting. The RSSI- and PRR-based logistic regression model outperformed the other two models, with an RMSE difference of 111–122%. These LQE models can be implemented on SMs or modems to monitor the reliability and efficiency of the AMI last-mile communication network.

Keywords: link quality estimation (LQE); advanced metering infrastructure (AMI); Wi-SUNs



Citation: Tangsunantham, N.; Pirak, C. Experimental Performance Analysis of Hardware-Based Link Quality Estimation Modelling Applied to Smart Grid Communications. *Energies* **2023**, *16*, 4326.
<https://doi.org/10.3390/en16114326>

Academic Editors: Abu-Siada Ahmed and David Dorrell

Received: 3 May 2023
Revised: 19 May 2023
Accepted: 24 May 2023
Published: 25 May 2023



Copyright: © 2023 by the authors. Licensee MDPI, Basel, Switzerland. This article is an open access article distributed under the terms and conditions of the Creative Commons Attribution (CC BY) license (<https://creativecommons.org/licenses/by/4.0/>).

1. Introduction

With the deployment of wireless sensor networks (WSN) and smart devices, the Internet of Things (IoT) has gained widespread adoption and replaced analog devices in several sectors, enabling more efficient data collection, analysis, and communication. This has led to increased efficiency and the ability to remotely real-time monitor and control various systems and processes, resulting in reduced costs and improved productivity. In the energy sector, the smart grid (SG), powered by the Industrial Internet of Things (IIoT), has improved the efficiency, reliability, and sustainability of electricity grids including real-time generation and distribution. The IIoT applications for the SG are more specialized for energy industrial use compared to the IoT, which collects and analyzes large amounts of data from the electricity grids, with the goal of improving the efficiency, reliability, and sustainability of the grids. Currently, many applications are connected to the electricity grid. For example, renewable energies (REs) such as solar rooftops or wind turbines are unstable electrical sources related to the weather conditions. Although energy storage systems can help improve the reliability of grids by smoothing out the fluctuations of a distribution generation system (DG), the cost of investing in energy storage systems is still high. Others, such as electric vehicles (EVs) and their chargers, which rely on the grids, can act as both the load and batteries. In order to improve the reliability and sustainability of the grid, the advanced metering infrastructure (AMI) system is integrated with the SG to realize the IIoT's capabilities. The AMI system establishes a robust two-way communication network between smart meters and utility control centers, providing significant benefits for utilities including labor cost savings, enhanced reliability, improved

power quality, better environmental sustainability, better consumption forecasting, and better detection of fraud. For consumers, the AMI system improves the consumption efficiency, detects electricity leakage, empowers decision-making, and aids in identifying theft incidents. These advancements optimize the operational efficiency within the utility sector, while offering cost savings and increased safety for consumers [1,2]. The AMI architecture demonstrates flexibility, which relies on the AMI functionality, communication technologies, and smart meter interoperability. Its core components include smart meters (SMs), communication networks, head-end systems (HESs), and meter data management systems (MDMSs). Some AMI systems also incorporate a data concentrator unit (DCU), as a gateway, to aggregate data from multiple smart meters and then transmit such data to the HES. The MDMS is responsible for managing, collecting, and storing smart meter data, as well as handling event filtering, load profile validation, data analytics, and policies such as virtual metering and load research. The HES acts as an interoperable link between the smart meters and the MDMS, with the MDMS providing the necessary application programming interface (API) to support multiple HES connections depending on the smart meter interoperability policy. The AMI system also enables the real-time collection and analysis of data from smart meters (SMs) and other devices, via last-mile communication networks.

Radio signals are typically corrupted by interference, noise, and multi-path fading, which affect the reliability and robustness [3] of the SMs' WSN. The SMs' radio frequency (RF)-mesh wireless networks are able to self-organize or self-heal the network characteristics such as node routing and node clustering [4]. An important factor of a flexible WSN is the link quality, which represents the reliability of the physical layer of the WSN. Link quality estimation (LQE) is the process of estimating the link quality in each hop in the WSN. An accurate LQE will enable the WSN to reroute the communication traffic through a different path or use a different frequency to avoid interference. LQE has a variety of link quality metrics as follows. The packet reception rate (PRR) is the most-straightforward metric of the link quality, which is the ratio of the number of successfully received packets and the number of transmitted packets. Nonetheless, it may not always provide an accurate representation depending on the window time it takes to obtain the data [5]. Alternative metrics are the signal-to-noise ratio (SNR), the received signal strength indicator (RSSI), and the link quality indicator (LQI), which are included in certain mapping relationships with the PRR for rapidly estimating the link quality. Techniques that use physical hardware indications to estimate the link quality are commonly referred to as a hardware-based LQE. Several studies have used the hardware-based LQE in multiple conditions and environments, such as the industrial environment and smart distribution grids; however, they have not focused on the SMs' RF-mesh WSN for AMI applications. Wireless smart utility networks (Wi-SUNs) are a low-power, wide-area networking (LP-WAN) standard designed for seamless connectivity in smart utility networks, e.g., smart municipalities, city infrastructure monitoring, and AMI last-mile communication. Wi-SUNs are based on the Zigbee (IEEE 802.15.4) standard and include amendments for the physical layer (PHY) (IEEE 802.15.4g) [6] and the MAC layer (IEEE 802.15.4e) [7]. For the network layer, the Wi-SUN standard's implementation utilizes the IPv6 routing protocol for low-power and lossy networks (RPL) as its routing protocol [8]. In addition, the IEEE 802.15.4g Wi-SUN PHY supports multi-region operations and operational frequency bands specific to each country [9], which are useful factors for the link quality estimation and routing protocol. At the network layer, the RPL facilitates the creation of routes and the optimal distribution of routing information among nodes. The RPL is an IPv6 routing protocol designed for low-power and high-throughput networks by utilizing distance vectors [10]. A highly efficient, accurate, and adaptive framework for LQE is vital to enable routing protocols to select the optimal routing path amidst varying network conditions. It is widely recognized that transmitting data through high-quality links could enhance the network throughput by minimizing the packet losses and extending the network lifespan by reducing the need for retransmissions. Furthermore, link quality estimation plays

a critical role in detecting dynamic link behaviors and maintaining topological stability. For example, LQE is essential for identifying short-lived high-quality links or predicting short-term variations in link quality. The RL-based link quality estimation (LQE) employs reinforcement learning (RL) to enhance the measuring probe used in the RPL, in which the RL-based link quality estimation (LQE) enhances the tradeoff between the packet delivery ratio (PDR) and the control overhead by imposing more control overhead [11,12]. AI-driven AMI network planning with DA-based information and a link-specific propagation model (AIDA) utilizes a minimum-spanning-tree (MST)-based technique to analyze multi-hop connectivity, aiming to minimize the number of connections to be evaluated. The AIDA analysis relies on the LQE between smart meters (SMs) and key device positions. The AIDA has been employed in large-scale projects, encompassing over 230,000 smart meters in the AMI planning of southern Brazil [8]. The main contribution of this article includes the evaluation of LQE models, which are compatible with the Wi-SUN and Thailand's regulations, including the SNR-based model, the mapping model, and the RSSI- and PRR-based logistic regression model. Thailand's smart grid development master plan [13], the replacement of electromechanical and automatic meter reading (AMR) meters with smart meters, is currently in progress. The most-accurate LQE model can improve the efficiency and reliability of the network planning, routing, monitoring, and operation for AMI last-mile communication networks.

This article is organized as follows. The related works on the LQE model for AMI last-mile communication networks are presented in Section 2. In Section 3, the LQE modeling methodology and results are shown. In Section 4, the discussion of the hardware-based LQE for different methods is presented. Finally, the conclusions and the future works are presented.

2. Related Works

2.1. Link Quality Estimation for WSNs

In order to improve the total performance of a WSN, LQE is a significant parameter for the PHY layer information, which is related to multiple link quality metrics. The LQE can be estimated by the observation and prediction windows. The observation window is a time window $[t_0, t_1]$ of the received packets' information that is collected by a node. The prediction window is a time window $[t_1, t_2]$ of the delivery link, which is defined after the observation link [14]. Larger observation windows can improve the accuracy of link capacity prediction; however, there is a tradeoff for LQE with increased energy consumption. Therefore, an efficient LQE design should be subject to minimizing both the time window and memory requirements, while maintaining a high precision. The LQE metrics are classified into hardware-based LQE and software-based LQE.

The upper layer information is used for the software-based LQE, such as the PRR-based model, the requested-number-of-packets (RNP)-based model, the score-based model, and the PDR-based model [15]. The efficiency of the PRR-based LQE is greatly related to the time window's size adjustment. This is rapidly and accurately executed when the PRR is extremely high or low, even though the window mean with the exponentially weighted moving average (WMEWMA) filter and the Kalman filter are applied to improve the speed. However, they experience a tradeoff with a high computational complexity. The required-number-of-packets (RNP)-based LQE counts the average number of packet transmissions or retransmissions required before a successful reception. It performs better than the PRR-based model; however, it is very unstable. The score-based LQE gives a score, which is defined within a certain range without the knowledge of the physical information, e.g., a packet reception or a packet retransmission. Several studies on score-based LQE models have presented high memory requirements and a complex process [5]. The packet delivery ratio (PDR) is a metric that measures the percentage of packets that are successfully delivered to their intended destination, while the packet reception rate (PRR) considers only the successful receptions. The PDR-based LQE was presented by [15], which uses the RSSI and machine learning (ML) techniques, such as K-nearest neighbor (KNN) and

long short-term memory (LSTM), to predict the link quality, for which high memory and computation are required.

The hardware-based LQE does not require high computational resources, and the PHY parameters can be obtained from the hardware register of the node devices, which have high agility and a low overhead. There are several hardware-based LQE metrics such as mapping models, the SNR, the RSSI, and the LQI [16]. The mapping models present the estimation of the PRR at different communication distances according to the LQE of each node. In [17], the authors proposed a mapping model that integrates the theoretical PRR model and log-normal path loss model for the PRR and communication distances associated with an industrial environment. In [18], the mapping model for the WSN in a residential area of a smart distribution grid was proposed; however, this WSN uses a Zigbee network, which has a different signal behavior from the AMI last-mile Wi-SUN. Therefore, the mapping model for the AMI last-mile Wi-SUN was included in this study by incorporating the log-normal shadowing path loss model to estimate the PRR. In the SNR-based LQE model, the theoretical bit error rate (BER) model and the SNR of the modulation techniques can be used to calculate the PRR. The theoretical model of a direct sequence spread spectrum offset quadrature phase shift keying (DSSS-OQPSK) modulation, which is based on a Zigbee standard, was used for the PRR estimation in [19,20]. In the IEEE 802.15.4g Wi-SUN standard, multi-region operations and operation-specific frequency bands are allowed, which are multi-rate frequency shift keying (MR-FSK) modulation, multi-rate orthogonal frequency division multiplexing (MR-OFDM) modulation, multi-rate offset quadrature phase shift keying (MR-OQPSK), the sub-GHz band, and the industrial, scientific, and medical (ISM) band [21]. The SNR-based LQE model for the AMI last-mile network is formulated by the theoretical BER of the MR-FSK modulation for the PRR estimation. The RSSI and LQI are widely used in the hardware-based LQE, which are related to the PRR. The RSSI is a measurement of the power of the received signal in decibel-milliwatts (dBm). The LQI is a measurement of the quality of the received signal. The LQI and PRR correlation can be more effective than the RSSI and SNR correlation of the PRR, which is shown by the fluctuation ranges of the RSSI and SNR when the node's environment changes [20,22]. However, the LQI has a different definition and implementation depending on specific chip vendors [16]. The LQIs from different vendors will be an issue for the SMs' interoperability network. Therefore, the RSSI- and PRR-based model is a good choice for the LQE model. Although the background noise in different environments affects the LQE accuracy, the RSSI- and PRR-based logistic regression model was worth studying in this study for the AMI last-mile network. In addition, three LQE models are compatible with the AMI Wi-SUN standard and Thailand's regulations.

2.2. Wi-SUN (IEEE 802.15.4g) PHY Layer

The limitations of Zigbee's 2.4 GHz frequency and applications, which are used for multiple purposes such as smart homes, smart buildings, etc., are extremely shared resources in the ISM band. As a result, the Wi-SUN is specifically designed for smart utility applications, i.e., an IIoT communication network, which is an alternative to the Zigbee standard, and it also includes the sub-GHz frequency band and multi-rate adjustability. The Wi-SUN was adopted and developed based on some aspects of Zigbee. The sub-GHz frequency bands have a longer wavelength, which allows for a longer communication range and better penetration through obstacles, such as walls and trees, much better than Zigbee's 2.4 GHz frequency. This is particularly useful for the last-mile communication in smart utility networks, where SMs' installation locations have experienced obstructions in urban and suburban areas. Additionally, the Wi-SUN's multi-rate adjustability is configurable for different environments and conditions; therefore, it can improve the AMI last-mile network's reliability and performance [23].

MR-OQPSK in the Wi-SUN is a part of the common characteristics shared with Zigbee, in which OQPSK is used; however, it has a PHR (PHY header) format, multiple data rates, and a multiplexed direct sequence spread spectrum (MDSSS) in the Wi-SUN. The data rates

of MR-OQPSK are between 6.25 and 500 kbps. MR-OFDM provides high data rates and interference resistance, which is the concept of OFDM, in which the information is spread into multiple sub-carriers within a data frame. The achievable data rate of MR-OFDM varies between 50 and 800 kbps, which is higher than MR-FSK and MR-OQPSK; however, there is a tradeoff with the high power consumption and complex circuitry requirements. MR-FSK is a popular PHY layer [7,24], which is used in many commercial applications due to its low complexity and good power efficiency. MR-FSK has a constant envelope of the signal, which makes it more energy efficient and supports multi-region operation. The PHY service data unit (PSDU) process has a forward error correction (FEC) as an option. The filtered MR-FSK, such as GFSK, meets the regulatory requirements of each region. The data rates of MR-FSK are between 5 and 400 kbps. In the AMI last-mile network, high efficiency, low complexity implementation, and interoperability are required. MR-FSK is the focus of this article, which was implemented in multiple regulated frequency bands and data rates supported by the AMI last-mile network. The MR-FSK multi-region operation of each region is shown in Table 1.

Table 1. MR-FSK multi-region operation of each region [24].

Regulatory Domain	Frequency Band (MHz)	Data Rates (kbps)
China	470–510, 779–787	50, 100, 200
Europe	863–870	50, 100, 200
U.S.	902–928	50, 150, 200
Korea	917–923.5	50, 150, 200
Japan	920–928, 950–958	50, 100, 200, 400
Worldwide	2400–2483.5	50, 150, 200

Currently, the number of energy meters to be installed in Thailand is around twenty-two million meters. The meter locations are situated in urban, suburban, and rural areas; however, the first pilot project of the SMs' deployment was launched in urban and suburban areas, such as in Bangkok and Pattaya city. Thailand's smart grid development master plan for 2015 to 2036 [13] intends to achieve smart grid transformation in four phases as follows: a preparation phase (2015–2016), a short-term phase (2017–2021), a middle-term phase (2022–2031), and a long-term phase (2032–2036). Nevertheless, the COVID-19 pandemic situation has delayed the current plan in the short-term phase. Currently, the electricity utilities have set up AMI pilot projects and required the frequency bands in the middle-term phase. The reserved unlicensed band for IoT applications in Thailand [25], which has been allocated as 920–925 MHz, is temporarily used in some AMI pilot projects. The radio frequency utilization for the development of the smart grid in Thailand, referring to a report published by the National Broadcasting and Telecommunications Commission (NBTC), Thailand [26], is well suited for the AMI last-mile Wi-SUN, as shown in Table 1 (Japan). The NBTC also suggests using the unlicensed bands (i.e., 433 MHz, 920–925 MHz, 2.4–2.5 GHz, and 5 GHz) for SG applications in Thailand; however, the dedicated frequency band (i.e., 442.5125–443.5125 MHz and 447.5125–448.5125 MHz) for SG applications was approved in 2019 [27], such as AMR/AMI, distribution automation, and microgrids. The MR-FSK multiple operation, which is compatible with the Wi-SUN for AMI application in Thailand, is given in Table 2. The alias is a representation of the MR-FSK operation under the NBTC regulations for a given transmit power and bandwidth [25–27]. The hardware-based LQE based on the MR-FSK operations is useful for the AMI last-mile network management in Thailand. In addition, the network can well maintain the quality of service (QoS) of IIoT network communication.

Table 2. The studied data rates and frequency bands of the 2FSK PHY layer in Thailand.

Frequency (MHz)	Data Rate (kbps)	Channel Spacing (kHz)	Alias	Transmit Power (dBm)
433.92	50	200	2FSK-433-50	10
	100	400	2FSK-433-100	10
	200	400	2FSK-433-200	10
443	50	200	2FSK-443-50	10
	100	400	2FSK-443-100	10
	200	400	2FSK-443-200	10
448	50	200	2FSK-448-50	10
	100	400	2FSK-448-100	10
	200	400	2FSK-448-200	10
923	50	200	2FSK-923-50	20
	100	400	2FSK-923-100	20
	150	400	2FSK-923-150	20
	200	400	2FSK-923-200	20
2440	50	200	2FSK-2440-50	5
	150	400	2FSK-2440-150	5
	200	400	2FSK-2440-200	5

3. LQE Modeling Methodology and Results

3.1. Experimental Setup

The tropical residential housing in Nonthaburi Province, Thailand, served as the experimental area for this study, as shown in Figure 1. This area is representative of the suburban AMI last-mile WSN. It also features a similar pattern of houses located along the side of the road. The presence of surrounding trees and objects, such as moving vehicles, can produce interference and multipath fading, making this area suitable for modeling the LQE in realistic conditions. The utility's energy meters in Thailand are owned and installed by either the Metropolitan Electricity Authority (MEA) or the Provincial Electricity Authority (PEA), depending on the regions. These meters are located on utility poles in the residential housing developments. The LAUNCHXL-CC1352P development board from Texas Instruments is equipped with a programmable multi-band radio, and it supports various protocols, as shown in Figure 2a. It is capable of operating at both sub-GHz and 2.4 GHz frequencies, allowing for compatibility with the IEEE 802.15.4g Wi-SUN. The Wi-SUN development board measures the PHY parameters, such as the RSSI, and collects the received packets into the mini personal computer (PC), which was loaded in a backpack, via an RS-232 serial port interface. The Wi-SUN development board, which is the receiver node, was installed on top of a small pole, which was stuck to the backpack, as shown in Figure 2b.

**Figure 1.** The experimental residential area.

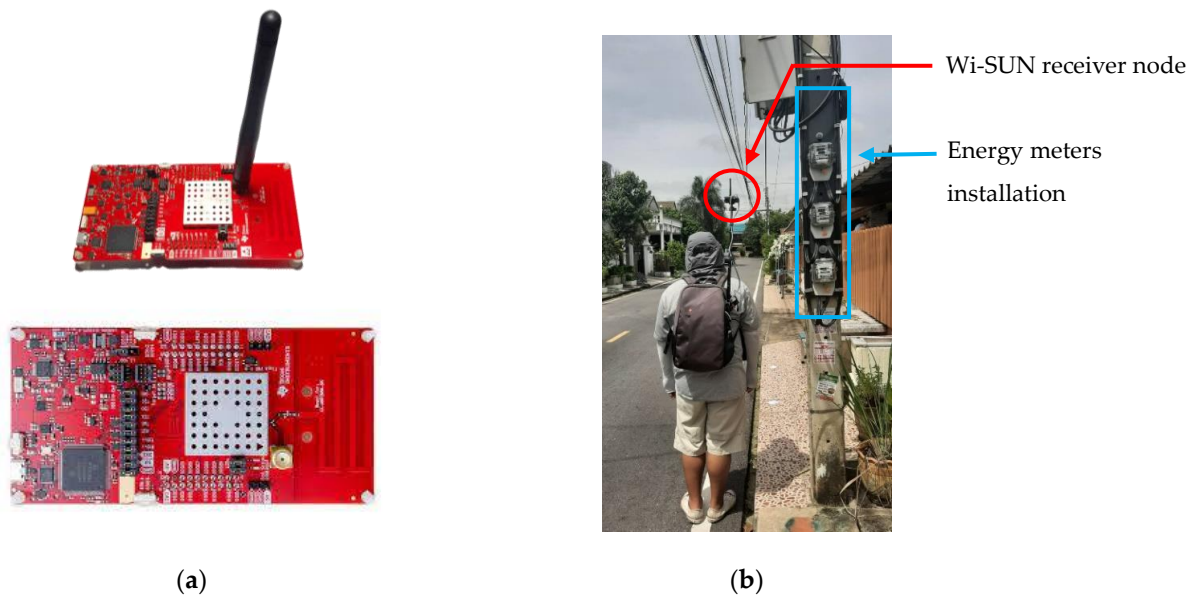


Figure 2. (a) IEEE 802.15.4g Wi-SUN development board model LAUNCHXL-CC1352P; (b) IEEE 802.15.4g Wi-SUN receiver node on the backpack and energy meters on the pole.

In order to simulate the position of a data concentrator unit (DCU) on a utility's low-voltage pole along the side of a street, a transmitter conforming to the IEEE 802.15.4g standard was installed at about four meters above the ground on a tripod. The Wi-SUN receiver node on the backpack was mounted at about two meters above the ground, simulating the installation height of an energy meter. The transmitter sends 255-byte packets at a periodic interval of 500 ms for all aliases, shown in Table 2, without the use of forward error correction (FEC). The experimental setup parameters are presented in Table 3. Each packet contained a packet counter number stamped in the transmit payload. The Wi-SUN receiver captures all received packets, which include the packet counter number, the random data, and the RSSI value measured at the receiver. These data were stored in a mini-PC, as shown in Figure 2b.

Table 3. System specification in the experiment.

Specification	Value	Unit
WSN standard	IEEE 802.15.4g-2012 (Wi-SUN)	-
Modulation, frequency, data rate, and transmit power	All aliases in Table 2	-
Antenna gain	2	dBi
DCU simulation installation height (Tx)	4	m
SM simulation installation height (Rx)	2	m
Payload size	255	bytes
Tx packet interval	500	ms

3.2. LQE Modeling for AMI Last-Mile Wi-SUN

3.2.1. SNR-Based Model

The SNR-based model has a modeling method that uses the theoretical BER of the modulation and the noise floor in each location to determine the packet reception rate (PRR) related to the SNR and RSSI for LQE. In this study, 2FSK modulation was chosen in the IEEE802.15.4g Wi-SUN PHY layer. The signal-to-noise ratio (SNR) of the 2FSK modulation, which uses two orthogonal frequencies to represent 0 and 1, impacts the bit error rate (BER) in the receive packets. The BER of 2FSK (P_{2FSK}) is the complementary error function (erfc) of the ratio of the energy per bit to the noise power spectral density (E_b/N_0), in the presence of an additive white Gaussian noise (AWGN) channel, as determined in

Equation (1) [28]. In addition, the Wi-SUN PHY layer provides the multi-data rate R and, thus, the relation of the SNR and multi-data rate recalls in Equation (2) [29], in which B denotes the channel bandwidth of the alias in Table 2. Therefore, the BER of 2FSK for the Wi-SUN is presented in Equation (3) in dBm.

$$P_{2FSK} = \frac{1}{2} \operatorname{erfc} \left(\sqrt{\frac{\operatorname{SNR}}{2}} \right) \quad (1)$$

$$\operatorname{SNR} = \frac{E_b}{N_0} \times \frac{R}{B} \quad (2)$$

$$P_{2FSK} = \frac{1}{2} \operatorname{erfc} \left(\sqrt{\frac{E_b}{2N_0} \times \frac{R}{B}} \right) \quad (3)$$

The relationship of the PRR and P_{2FSK} follows Equation (4), in which l denotes the value of the bits per frame, to arrive at:

$$\operatorname{PRR} = (1 - P_{2fsk})^l \quad (4)$$

The plot of the PRR with various data rates of the Wi-SUNs is shown in Figure 3, which illustrates that the PRRs for a group of data rates of 50 and 100 kbps are higher than the data rates of 150 and 200 kbps, respectively. The RSSI can be used to determine the received signal power (P_{rx}) and the noise floor at the receiver. The noise floor (NF) is the level of background noise present at the Wi-SUN receiver node. It can also be taken into consideration when interpreting the RSSI value, as determined in Equation (5). The noise floor significantly impacts the performance of the WSN and the link quality, which is measured using a Wi-SUN receiver node, rather than being taken by external devices such as spectrum analyzers. The receiver node receives the frequency band of all aliases in Table 2. The observed noise floors experienced in the area are presented in Table 4. In addition, the relationship between the RSSI, P_{rx} , and NF can be expressed as

$$\operatorname{RSSI} = P_{rx} + \operatorname{NF} \quad (5)$$

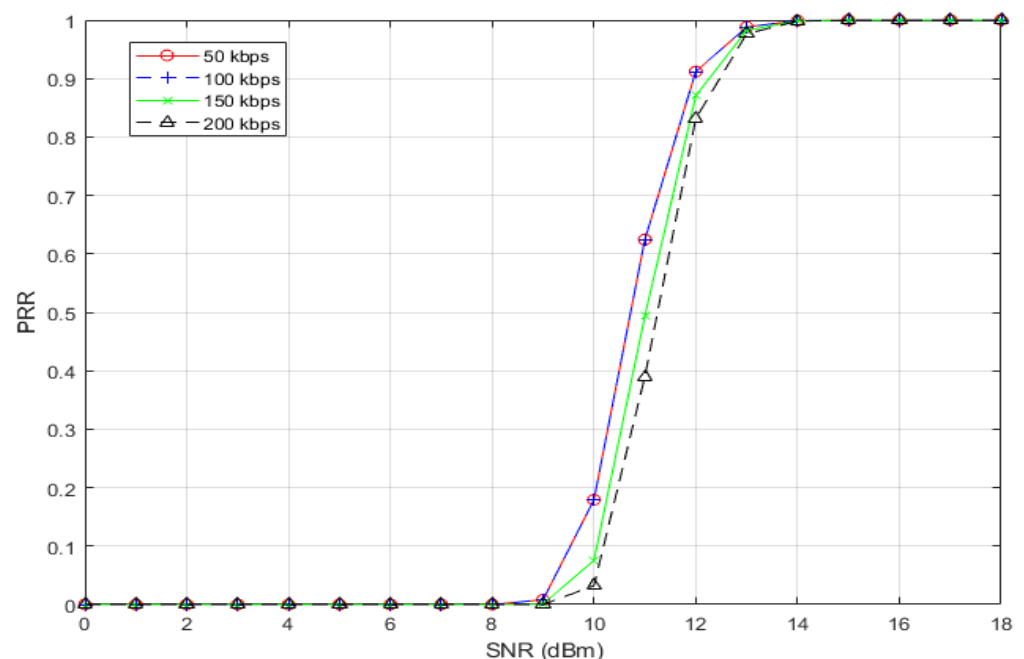


Figure 3. PRR of 2FSK with various data rates (50, 100, 150, 200 kbps) in Wi-SUNs.

Table 5. The distance between a Wi-SUN transmitter and a receiver node.

-	P1	P2	P3	P4	P5	P6	P7
Distance from transmitter to receiver (m)	10	20	40	60	80	85	105

Table 6. Linear regression parameters of Equation (8).

Alias	a	n
2FSK-433-50	-0.21	-13.12
2FSK-433-100	-0.22	-13.29
2FSK-433-200	-0.23	-15.67
2FSK-443-50	-0.51	-36.39
2FSK-443-100	-0.43	-30.73
2FSK-443-200	-0.38	-28.29
2FSK-448-50	-0.26	-16.84
2FSK-448-100	-0.25	-16.45
2FSK-448-200	-0.302	-20.68
2FSK-923-50	-0.214	-12.107
2FSK-923-100	-0.218	-10.59
2FSK-923-150	-0.221	-10.58
2FSK-923-200	-0.217	-10.25
2FSK-2440-50	-0.217	-14.562
2FSK-2440-150	-0.208	-12.61
2FSK-2440-200	-0.2107	-12.69

The PRR based on the mapping model is determined by $P_{2\text{FSK}}$ in Equation (6), which is then substituted into Equation (4), to arrive at

$$\text{PRR}_{\text{Mapping model}} = \left(1 - \frac{1}{2} \operatorname{erfc} \left(\sqrt{\frac{1}{2} \times \frac{B}{R} \times 10^{(\text{RSSI}-\text{NF})/10}} \right) \right)^l \quad (9)$$

3.2.3. RSSI- and PRR-Based Logistic Regression Model

A disadvantage of using the PRR as a metric for LQE is that its performance depends on the size of the time window, as described in Section 2.1. Additionally, the single RSSI value, which is contained in each received packet, tends to fluctuate in different received packets. Therefore, the logistic regression model was used to simplify the RSSI and PRR relationship. From Equations (3) and (4), the PRR is related to the BER, when the BER is determined by the received packets, which were recorded on the mini-PC for all aliases. The RSSI is also tagged with the received packet. Logistic regression is a statistical model that is used to predict the probability of an event occurring, given a set of independent variables. The Sigmoid-curve-fitting method is used to find the model that minimizes the root-mean-squared error (RMSE). The Sigmoid function is presented in Equation (10). Logistic regression was used to fit the PRR based on the larger amount of data. The Wi-SUN receiver node normally receives and records continuous packets sent by the transmitter. There were more than 2000 recorded received packets in each alias. The distance between the Wi-SUN transmitter and measurement points was around 5 to 80 m. The measurement points are shown in Figure 5. The RSSI- and PRR-based logistic regression model is described in Equation (11),

$$S(x) = \frac{1}{1 + e^{-x}} = \frac{e^x}{e^{-x} + 1} \quad (10)$$

$$\text{PRR}_{\text{RSSI and PRR based model}} = 1 / (1 + \exp(-K(\text{RSSI} + Z))) \quad (11)$$

where K and Z are the Sigmoid-curve-fitting parameters.

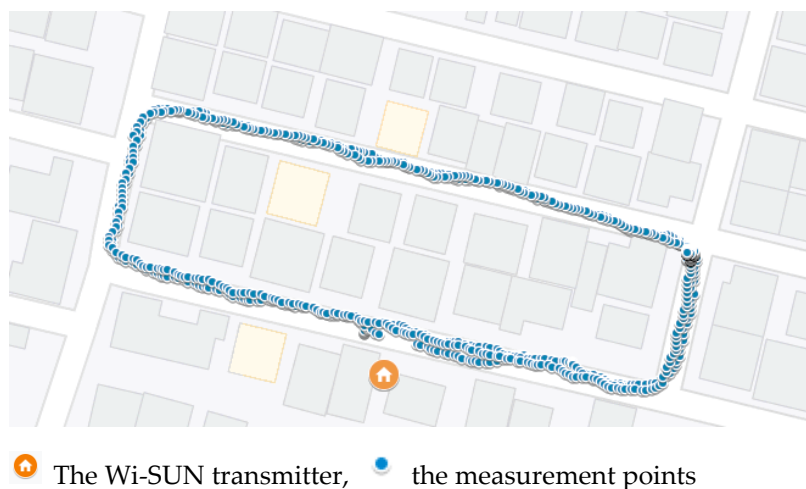


Figure 5. The Wi-SUN transmitter and the measurement points in the experiment area for the RSSI- and PRR-based logistic regression model.

The logistic regression model for the RSSI and PRR in the area is presented by the Sigmoid-curve-fitting parameters, i.e., K and Z , as shown in Table 7.

Table 7. Sigmoid-curve-fitting parameters of Equation (11).

Alias	K	Z
2FSK-433-50	1.086	106
2FSK-433-100	1.135	103
2FSK-433-200	0.9509	100
2FSK-443-50	0.4518	95
2FSK-443-100	0.503	93
2FSK-443-200	0.451	89
2FSK-448-50	0.6831	106
2FSK-448-100	1.228	103
2FSK-448-200	0.9697	100
2FSK-923-50	0.3528	105
2FSK-923-100	0.3939	103
2FSK-923-150	0.691	98
2FSK-923-200	0.7784	97
2FSK-2440-50	0.07904	55
2FSK-2440-150	0.08335	72
2FSK-2440-200	0.08346	79

3.3. Experimental Results

In Section 3.2, three LQE models are formulated, the SNR-based model, the mapping model, and the RSSI- and PRR-based logistic regression model. These models present the RSSI and PRR relationship taken from different hardware-based LQE metrics, and they are compatible with the AMI last-mile Wi-SUN in Thailand. The root-mean-squared error (RMSE), which determines the difference between the predicted value obtained from the models and the empirical value in a dataset obtained from the experiment, is expressed as Equation (12). The RMSE is commonly used as a metric for evaluating the performance of models. The empirical values are the RSSI and PRR. The PRR is determined by the P_{2FSK} of all received packets in each alias.

$$RMSE = \sqrt{\frac{\sum_{i=1}^N (\mu_{emp} - \mu_{model})^2}{N}} \quad (12)$$

where μ_{emp} denotes the PRR empirical values, μ_{model} denotes the PRR hardware-based LQE model values, and N denotes the number of samples used. The results of the RMSE and RMSE difference (%) are presented in Table 7, which presents the performance of each model and the RSSI and PRR relationship in various groups of frequencies, including the 433.92, 443, 448, 923, and 2440 MHz MR-FSK operations, as shown in Figures 6–10, respectively. The RMSE difference (%) is the difference between the RMSE of the RSSI- and PRR-based logistic regression model and the two other models.

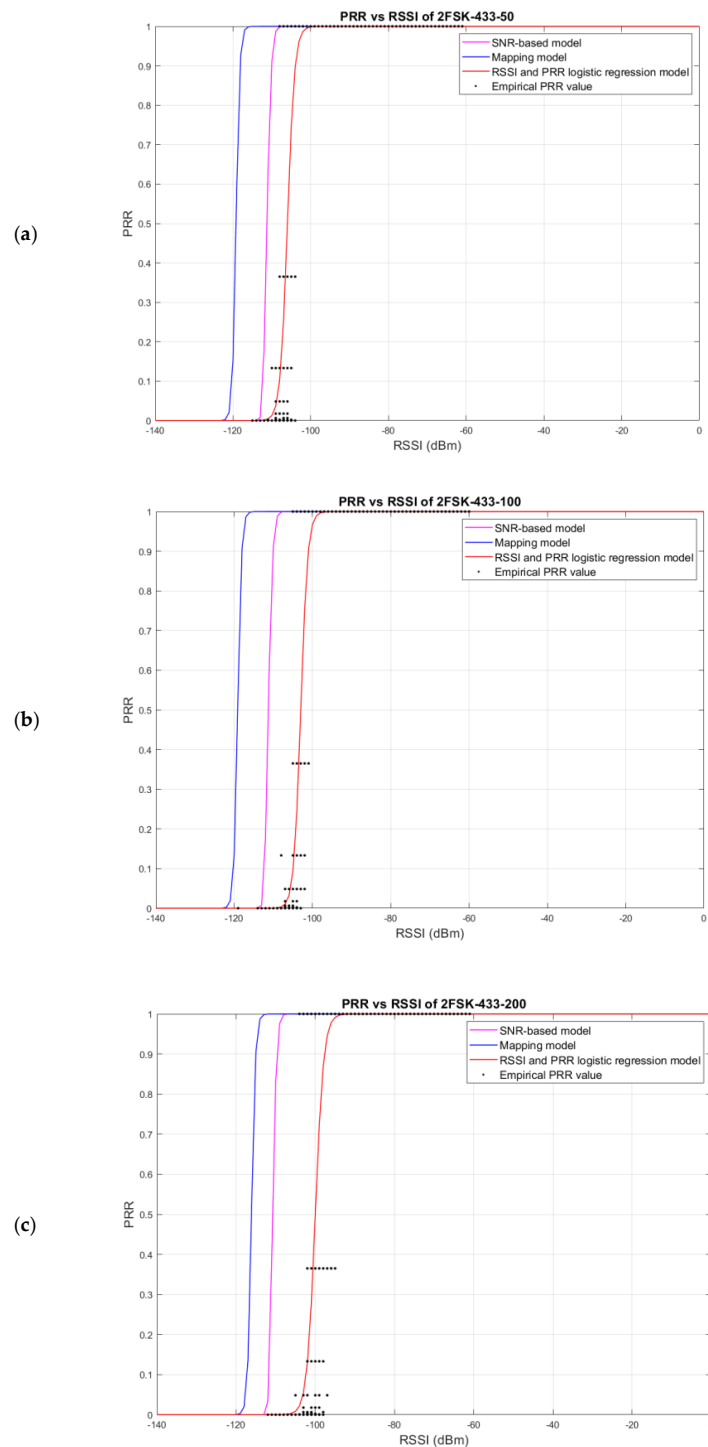


Figure 6. The plot of the LQE (PRR) versus RSSI (dBm) relation of different aliases: (a) 2FSK-433-50, (b) 2FSK-433-100, and (c) 2FSK-433-200.

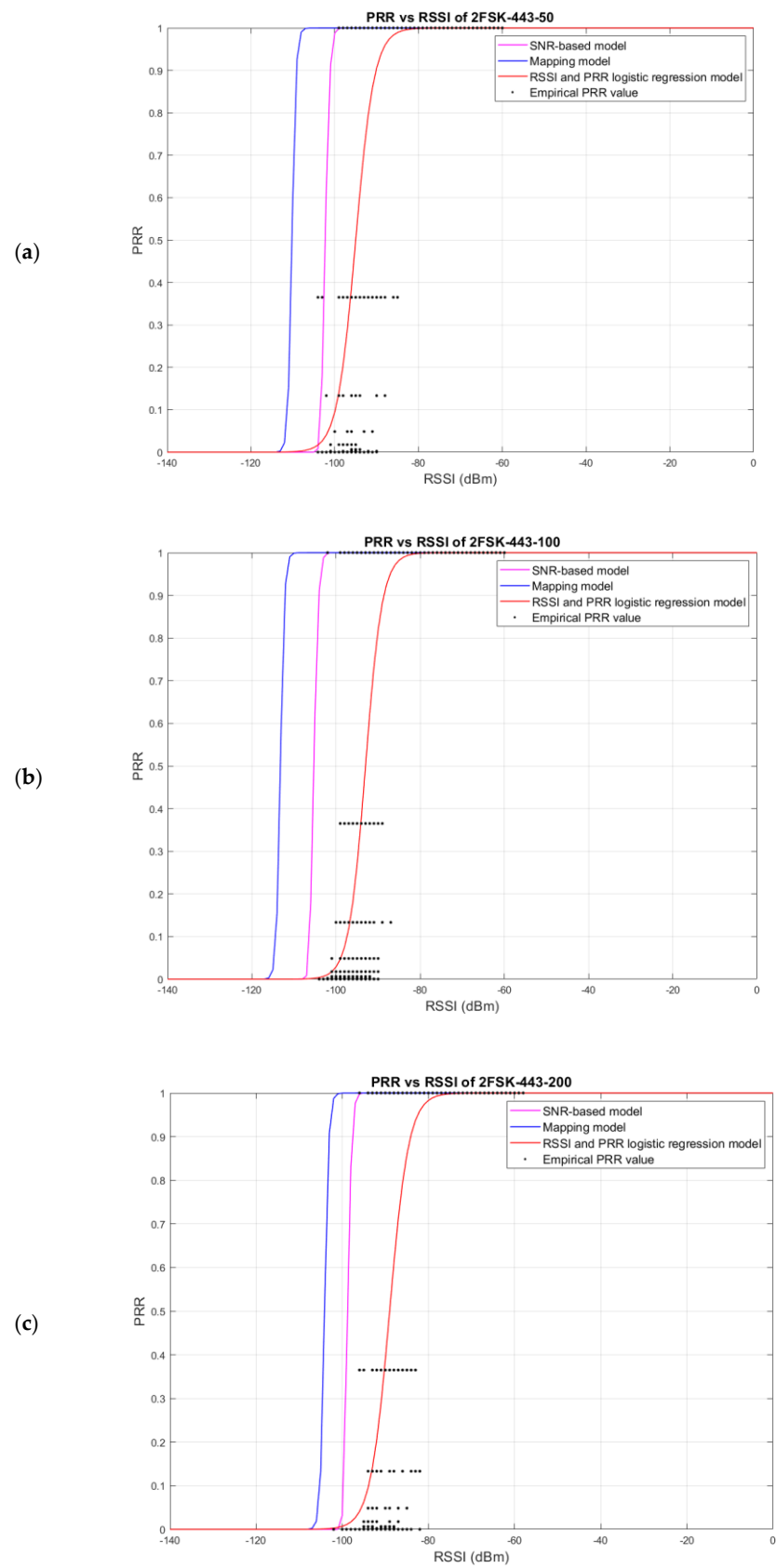


Figure 7. The plot of the LQE (PRR) versus RSSI (dBm) relation of different aliases: (a) 2FSK-443-50, (b) 2FSK-443-100, and (c) 2FSK-443-200.

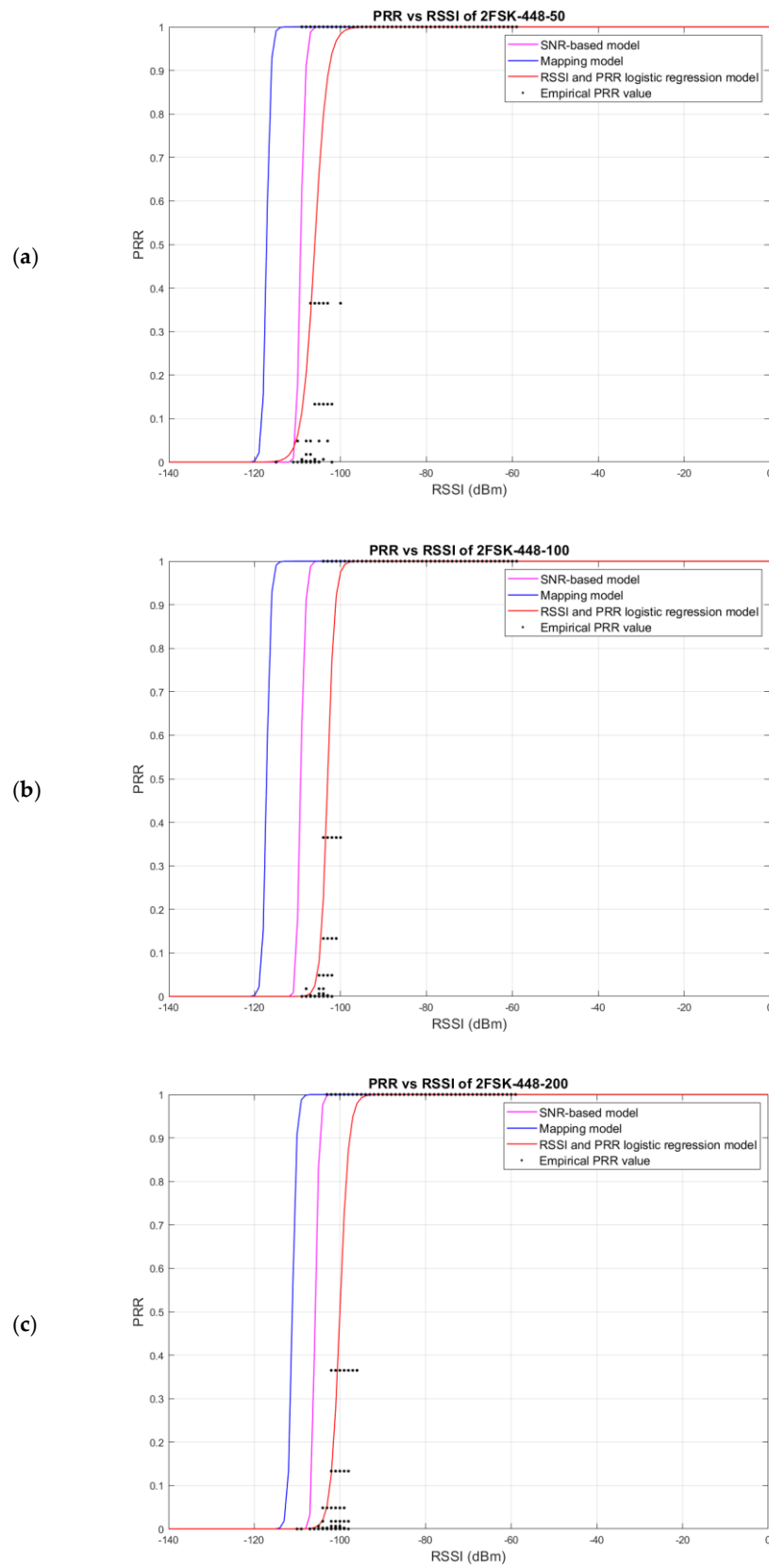


Figure 8. The plot of the LQE (PRR) versus RSSI (dBm) relation of different aliases: (a) 2FSK-448-50, (b) 2FSK-448-100, and (c) 2FSK-448-200.

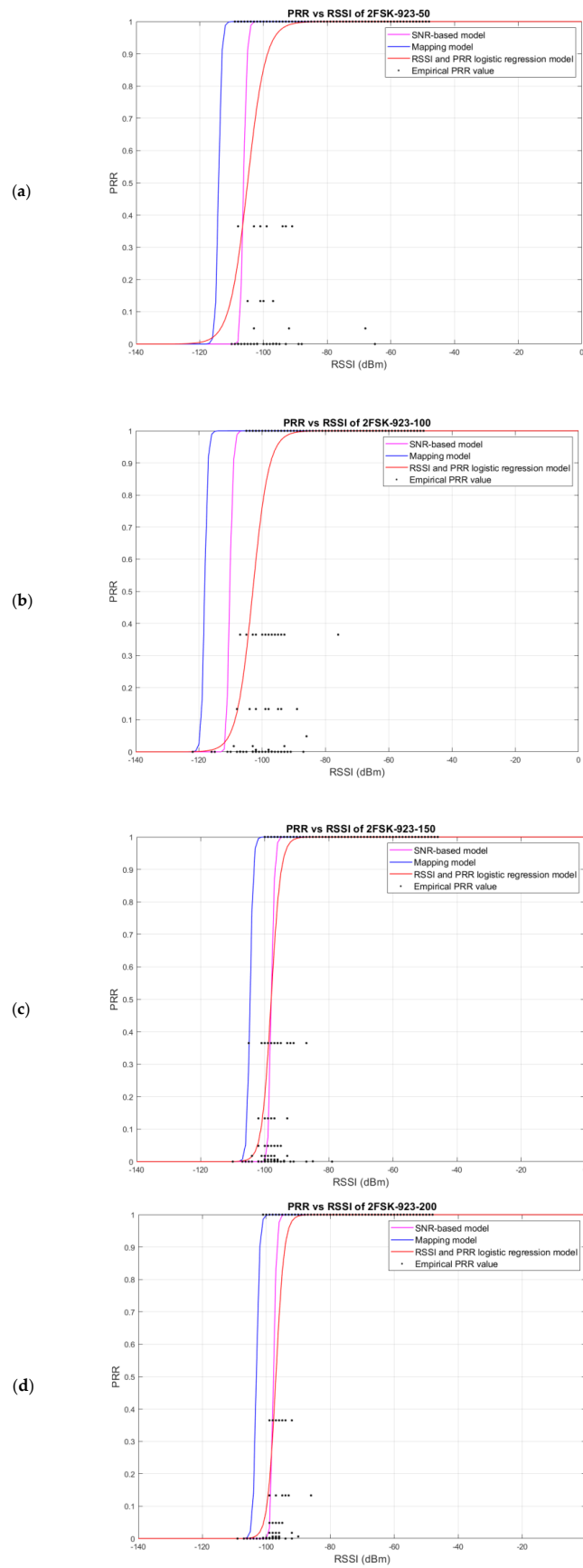


Figure 9. The plot of the LQE (PRR) versus RSSI (dBm) relation of different aliases: (a) 2FSK-923-50, (b) 2FSK-923-100, (c) 2FSK-923-100, and (d) 2FSK-923-200.

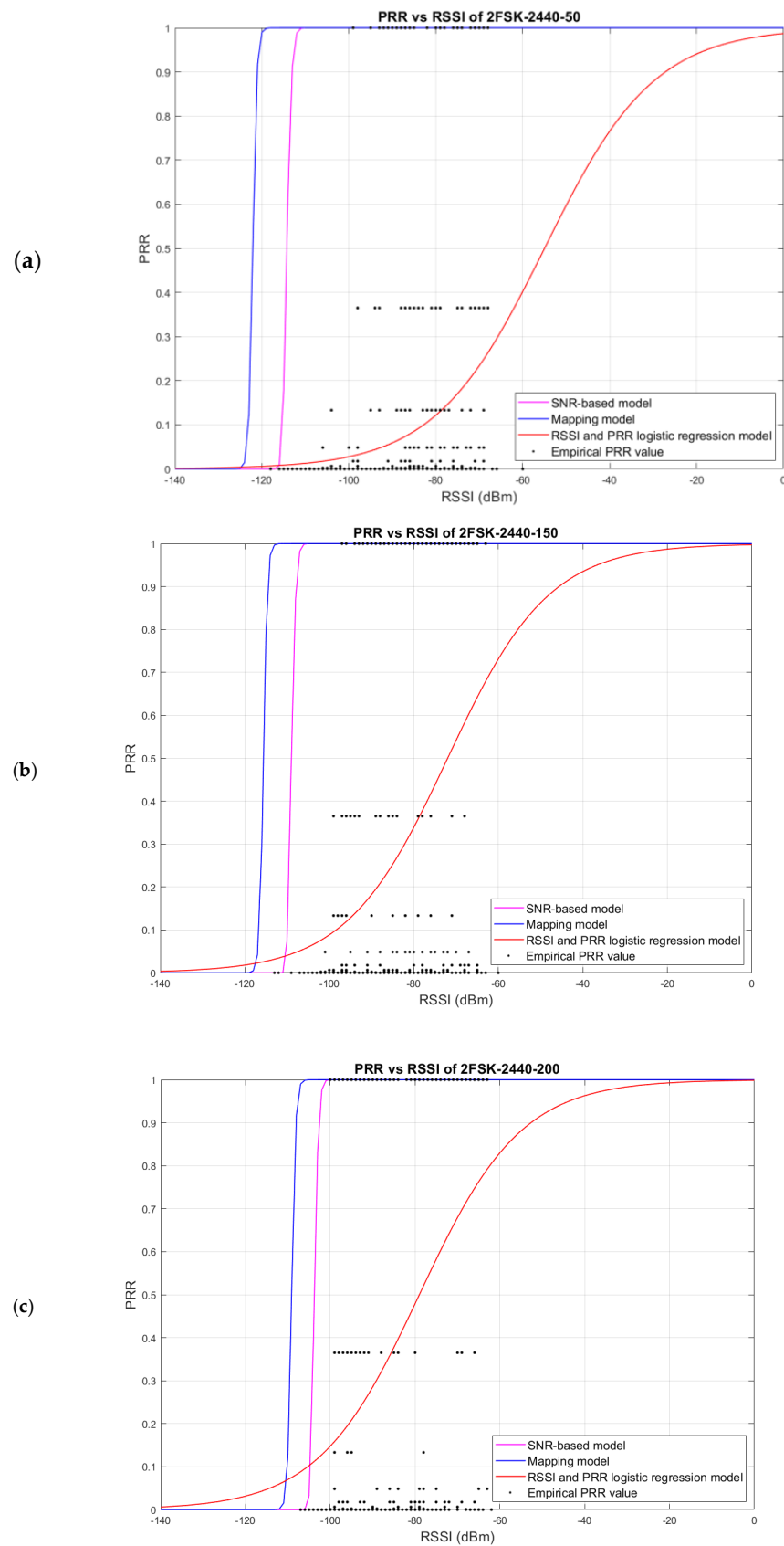


Figure 10. The plot of the LQE (PRR) versus RSSI (dBm) relation of different aliases: (a) 2FSK-2440-50, (b) 2FSK-2440-150, and (c) 2FSK-2440-200.

4. Discussion and Future Work

In this study, the accuracy of the PRR estimation, a key metric for link quality estimation (LQE), was evaluated using three hardware-based LQE models, the SNR-based model, the mapping model, and the RSSI- and PRR-based logistic regression model. The parameters for the mapping model and RSSI- and PRR-based logistic regression model are presented in Tables 6 and 7, respectively. The results, presented in Section 3.3 and summarized in Table 8, demonstrated that these models were effective for the PRR estimation in an AMI last-mile Wi-SUN, and they were compliant with Thailand's regulations. The performance of the LQE models was assessed by using the root-mean-squared error (RMSE) and compared to the PRR empirical value obtained from the received packets. The results are plotted in Figures 6–10, for the SNR-based model, the mapping model, and the RSSI- and PRR-based logistic regression model. Figures 6–8 show that the LQEs obtained from the SNR-based model and the RSSI- and PRR-based logistic regression model were close when using the 433 MHz unlicensed band and the 443 and 448 MHz licensed bands for Thailand's smart grid applications. Additionally, they were even closer in the 923 MHz reserved unlicensed band for IoT applications in Thailand, which is temporarily used in some AMI pilot projects. In contrast, Figure 10 indicates a significant difference between the LQEs from the SNR-based model and the RSSI- and PRR-based logistic regression model in the 2440 MHz unlicensed band. This discrepancy in the PRR empirical values can be attributed to frequency sharing with other applications, particularly in the context of AMI application within the 2440 MHz unlicensed band.

Table 8. The evaluation of the hardware-based LQE models.

Number	Alias	RSSI- and PRR-Based Model	SNR-Based Model		Mapping Model	
		RMSE	RMSE	RMSE Difference (%) ¹	RMSE	RMSE Difference (%) ²
1	0.1467	0.1467	0.3512	139%	0.3754	156%
2	0.1464	0.1464	0.4271	192%	0.4408	201%
3	0.1825	0.1825	0.4287	135%	0.4329	137%
4	0.2407	0.2407	0.4374	82%	0.4548	89%
5	0.2915	0.2915	0.6580	126%	0.6582	126%
6	0.2285	0.2285	0.4755	108%	0.4907	115%
7	0.1614	0.1614	0.2427	50%	0.2765	71%
8	0.1377	0.1377	0.3390	146%	0.3507	155%
9	0.1725	0.1725	0.3718	116%	0.3894	126%
10	0.1379	0.1379	0.1524	10%	0.1700	23%
11	0.1378	0.1378	0.1798	30%	0.1869	36%
12	0.1479	0.1479	0.1610	9%	0.2382	61%
13	0.1496	0.1496	0.1673	12%	0.2359	58%
14	0.2114	0.2114	0.9534	351%	0.9590	354%
15	0.3765	0.3765	0.8549	127%	0.8578	128%
16	0.4255	0.4255	0.7660	80%	0.7858	85%
Total average ³		0.2059	0.4353	111%	0.4564	122%

¹ The RMSE Difference (%) is the difference between the RMSE of the RSSI- and PRR-based logistic regression model and the SNR-based model. ² The RMSE Difference (%) is the difference between the RMSE of the RSSI- and PRR-based logistic regression model and the mapping model. ³ The Total average is the average value (i.e., RMSE and RMSE Difference (%)) of such a model in all aliases.

The experimental results, as shown in Table 8, demonstrated that all three hardware-based LQE models performed well in the PRR estimation. The RSSI- and PRR-based logistic

regression model showed the highest performance, where the RMSE was the minimum, in particular in the 923 MHz licensed band for all data rates and the 448 MHz licensed band for a low data rate (50 kbps). The SNR-based model and the mapping model also demonstrated a fair performance, with the lowest and highest RMSE differences at 9% at 923 MHz and 354% at 2440 MHz, respectively, when compared to the RSSI- and PRR-based logistic regression model. The RMSEs of all three hardware-based LQE models were low in the 923 MHz licensed band, whereas the RMSEs of the 2440 MHz unlicensed band were high, related to the PRR empirical values' distribution, as shown in Figure 10. It was shown that the licensed band was more proper than the unlicensed band, which is very crowded by many wireless applications, for the AMI Wi-SUN in Thailand. The total average root-mean-squared error (RMSE) difference, which reflected the overall performance in all aliases compared to the RSSI- and PRR-based logistic regression model, showed that the SNR-based model had superior performance to the mapping model, i.e., 111% compared to 122%, respectively. In this study, the smart meters were installed outdoors on utility poles. In the case of meter installation in indoor positions, challenges arise in accurately evaluating and validating the path loss and LQE models. The factors such as a signal attenuation, multipath interference, signal reflection, interference from other devices, and the proximity to electrical equipment can significantly influence the reliability and accuracy of LQE models within indoor environments, which will be studied in the future work.

For the complexity analysis, the complexity of the algorithms varied among the different LQE models. The RSSI- and PRR-based logistic regression model exhibited the highest complexity, but it also achieved the highest accuracy, i.e., the minimum RMSE. This model calculates the PRR for each packet using logistic regression, contributing to its increased complexity. On the other hand, the mapping model was less complex than the RSSI- and PRR-based logistic regression model, but it had an inferior performance. Among them, the SNR-based model was the simplest, yet it performed close to the RSSI- and PRR-based logistic regression model in some frequency bands, i.e., 433, 443, 448, and 923 MHz frequency bands. However, in the presence of interference in the 2440 MHz unlicensed band, the RSSI- and PRR-based logistic regression model outperformed the SNR-based model. Moreover, this model is well suited for deployment in tropical residential areas characterized by surrounding trees and objects, representing suburban areas within the AMI network. A limitation of the proposed RSSI- and PRR-based logistic regression model is its high computational complexity, which may present challenges during practical implementations. However, despite this limitation, the model demonstrated exceptional accuracy performance. To mitigate the complexity issue, future research efforts will focus on the simplified methodologies. Furthermore, additional investigations can explore the generalizability of the model by conducting experiments in diverse environmental settings and considering factors such as interference mitigation techniques and antenna configurations.

5. Conclusions

In this paper, link quality estimation (LQE) was studied to assess the link quality in each hop of the Wi-SUN AMI last-mile communication network. In the AMI last-mile communication network, three hardware-based LQE models, the SNR-based model, the mapping model, and the RSSI- and PRR-based logistic regression model, were modeled and evaluated following Thailand's regulations. The performance of the LQE models was assessed using the RMSE of the PRR empirical values obtained from the received packets and the LQE models. The results showed that all three hardware-based LQE models had good performance with a small value of the RMSE; however, the RSSI- and PRR-based logistic regression model outperformed the SNR-based model, with an RMSE difference of 111%, and the mapping models, with an RMSE difference of 122%, respectively. The SNR-based model and the mapping model also demonstrated a fair performance, with the lowest and highest RMSE differences of 9% and 354%, respectively, when compared to the RSSI- and PRR-based logistic regression model. This LQE model can be implemented on

SMs or modems, for the purposes of reliably and efficiently monitoring the AMI last-mile communications. In addition, with the LQE information, the AMI last-mile network is able to reroute the traffic or use a different frequency to avoid interference accordingly.

Author Contributions: Conceptualization, N.T. and C.P.; methodology, N.T. and C.P.; software, N.T. and C.P.; validation, N.T. and C.P.; formal analysis, N.T. and C.P.; investigation, N.T. and C.P.; resources, N.T. and C.P.; data curation, N.T. and C.P.; writing—original draft preparation, N.T.; writing—review and editing, C.P.; visualization, C.P.; supervision, C.P.; project administration, C.P.; funding acquisition, C.P. All authors have read and agreed to the published version of the manuscript.

Funding: This research was funded by King Mongkut’s University of Technology North Bangkok—Contract No. KMUTNB-61-PHD-007.

Data Availability Statement: Publicly available datasets were analyzed in this study. These data can be found here: <https://github.com/deepeed/datasets-LQEModel-energies2023>, accessed on 3 May 2023.

Conflicts of Interest: The authors declare no conflict of interest.

References

1. Lloret, J.; Tomas, J.; Canovas, A.; Parra, L. An Integrated IoT Architecture for Smart Metering. *IEEE Commun. Mag.* **2016**, *54*, 50–57. [[CrossRef](#)]
2. Saleem, Y.; Crespi, N.; Rehmani, M.H.; Copeland, R. Internet of Things-Aided Smart Grid: Technologies, Architectures, Applications, Prototypes, and Future Research Directions. *IEEE Access* **2019**, *7*, 62962–63003. [[CrossRef](#)]
3. Boucetta, C.; Nour, B.; Mounghla, H.; Lahlou, L. An IoT Scheduling and Interference Mitigation Scheme in TSCH Using Latin Rectangles. In Proceedings of the 2019 IEEE Global Communications Conference (GLOBECOM), Waikoloa, HI, USA, 9–13 December 2019; pp. 1–6. [[CrossRef](#)]
4. Imran, R.; Odeh, M.; Zorba, N.; Verikoukis, C. Quality of Experience for Spatial Cognitive Systems within Multiple Antenna Scenarios. *IEEE Trans. Wirel. Commun.* **2013**, *12*, 4153–4161. [[CrossRef](#)]
5. Baccour, N.; Koubâa, A.; Mottola, L.; Zúñiga, M.A.; Youssef, H.; Boano, C.A.; Alves, M. Radio link quality estimation in wireless sensor networks: A survey. *ACM Trans. Sen. Netw.* **2012**, *8*, 1–33. [[CrossRef](#)]
6. Mochizuki, K.; Obata, K.; Mizutani, K.; Harada, H. Development and field experiment of wide area Wi-SUN system based on IEEE 802.15.4g. In Proceedings of the 2016 IEEE 3rd World Forum on Internet of Things (WF-IoT), Reston, VA, USA, 12–14 December 2016; pp. 76–81. [[CrossRef](#)]
7. Chang, K.-H.; Mason, B. The IEEE 802.15.4g standard for smart metering utility networks. In Proceedings of the 2012 IEEE Third International Conference on Smart Grid Communications (SmartGridComm), Tainan, Taiwan, 5–8 November 2012; pp. 476–480. [[CrossRef](#)]
8. Mochinski, M.A.; Vieira, M.L.d.S.C.; Biczowski, M.; Chueiri, I.J.; Jamhour, E.; Zambenedetti, V.C.; Pellenz, M.E.; Enembreck, F. Towards an Efficient Method for Large-Scale Wi-SUN-Enabled AMI Network Planning. *Sensors* **2022**, *22*, 9105. [[CrossRef](#)] [[PubMed](#)]
9. Harada, H.; Mizutani, K.; Fujiwara, J.; Mochizuki, K.; Obata, K.; Okumura, R. IEEE 802.15.4g Based Wi-SUN Communication Systems. *IEICE Trans. Commun.* **2017**, *E100-B*, 1032–1043. [[CrossRef](#)]
10. Savitha, M.M.; Basarkod, D.P.I. A Comprehensive Survey on RPL: Evolution and Challenges. In Proceedings of the Second International Conference on Emerging Trends in Science & Technologies for Engineering Systems (ICETSE-2019), Chickballapur, India, 17–18 May 2019. [[CrossRef](#)]
11. Ancillotti, E.; Vallati, C.; Bruno, R.; Mingozzi, E. A reinforcement learning-based link quality estimation strategy for RPL and its impact on topology management. *Comput. Commun.* **2017**, *112*, 1–13. [[CrossRef](#)]
12. Seyfollahi, A.; Ghaffari, A. A Review of Intrusion Detection Systems in RPL Routing Protocol Based on Machine Learning for Internet of Things Applications. *Wirel. Commun. Mob. Comput.* **2021**, *2021*, 8414503. [[CrossRef](#)]
13. Ministry of Energy of the Kingdom of Thailand. Thailand Smart Grid Development Master Plan 2015 to 2036. Available online: https://www.eppo.go.th/images/Power/pdf/smart_gridplan.pdf (accessed on 3 May 2023).
14. Boano, C.A.; Zúñiga, M.A.; Voigt, T.; Willig, A.; Römer, K. The Triangle Metric: Fast Link Quality Estimation for Mobile Wireless Sensor Networks. In Proceedings of the 2010 19th International Conference on Computer Communications and Networks, Zurich, Switzerland, 2–5 August 2010; pp. 1–7. [[CrossRef](#)]
15. Boucetta, C.; Nour, B.; Cusin, A.; Mounghla, H. QoS in IoT Networks based on Link Quality Prediction. In Proceedings of the ICC 2021—IEEE International Conference on Communications, Montreal, QC, Canada, 14–23 June 2021; pp. 1–6. [[CrossRef](#)]
16. Liu, W.; Xia, Y.; Zheng, D.; Xie, J.; Luo, R.; Hu, S. Environmental Impacts on Hardware-Based Link Quality Estimators in Wireless Sensor Networks. *Sensors* **2020**, *20*, 5327. [[CrossRef](#)] [[PubMed](#)]
17. Sun, W.; Yuan, X.; Wang, J.; Li, Q.; Chen, L.; Mu, D. End-to-End Data Delivery Reliability Model for Estimating and Optimizing the Link Quality of Industrial WSNs. *IEEE Trans. Autom. Sci. Eng.* **2018**, *15*, 1127–1137. [[CrossRef](#)]

18. Sun, W.; Wei, L.; Wang, J.; Mu, D.; Li, Q.; Yuan, X. A Link Quality Estimation model of Wireless Sensor Networks for Smart Distribution Grid. *IFAC-PapersOnLine* **2015**, *48*, 432–437. [[CrossRef](#)]
19. Sun, W.; Lu, W.; Li, Q.; Chen, L.; Mu, D.; Yuan, X. WNN-LQE: Wavelet-Neural-Network-Based Link Quality Estimation for Smart Grid WSNs. *IEEE Access* **2017**, *5*, 12788–12797. [[CrossRef](#)]
20. Chang, X.; Huang, J.; Liu, S.; Xing, G.; Zhang, H.; Wang, J.; Huang, L.; Zhuang, Y. Accuracy-Aware Interference Modeling and Measurement in Wireless Sensor Networks. *IEEE Trans. Mob. Comput.* **2016**, *15*, 278–291. [[CrossRef](#)]
21. Muñoz, J.; Chang, T.; Vilajosana, X.; Watteyne, T. Evaluation of IEEE802.15.4g for Environmental Observations. *Sensors* **2018**, *18*, 3468. [[CrossRef](#)] [[PubMed](#)]
22. Jayasri, T.; Hemalatha, M. Link Quality Estimation for Adaptive Data Streaming in WSN. *Wirel. Pers. Commun.* **2017**, *94*, 1543–1562. [[CrossRef](#)]
23. Tangsunantham, N.; Pirak, C. Experimental Performance Analysis of Wi-SUN Channel Modelling Applied to Smart Grid Applications. *Energies* **2022**, *15*, 2417. [[CrossRef](#)]
24. Sum, C.S.; Zhou, M.T.; Kojima, F.; Harada, H. Experimental Performance Evaluation of Multihop IEEE 802.15.4/4g/4e Smart Utility Networks in Outdoor Environment. *Wirel. Commun. Mob. Comput.* **2017**, *2017*, 7137406. [[CrossRef](#)]
25. NBTC. Technical Standards of Telecommunication Equipment NTC TS 1033–2560 Radio Communication Radio Frequency Identification: The Frequency Range Is 920–925 MHz. Available online: https://infocenter.nbtc.go.th/storage/files/_contentSource_20171127_034358_1511772238958.PDF (accessed on 3 May 2023).
26. Benjapolakul, W. Radio Frequency Utilization for the Development of Smart Grids in Thailand. Available online: https://so04.tci-thaijo.org/index.php/NBTC_Journal/article/view/139500/115537 (accessed on 3 May 2023).
27. Fiscal Policy Research Institute Foundation. The Final Report of Spectrum Demand Study Project for Thailand. Available online: <https://www.nbtc.go.th/getattachment/Information/%E0%B8%9C%E0%B8%A5%E0%B8%81%E0%B8%B2%E0%B8%A3%E0%B8%A8%E0%B8%B6%E0%B8%81%E0%B8%A9%E0%B8%B2%E0%B8%A7%E0%B8%B4%E0%B8%88%E0%B8%B1%E0%B8%A2/39288/%E0%B8%A3%E0%B8%B2%E0%B8%A2%E0%B8%87%E0%B8%B2%E0%B8%99%E0%B9%82%E0%B8%84%E0%B8%A3%E0%B8%87%E0%B8%81%E0%B8%B2%E0%B8%A3-Spectrum-Outlook.pdf.aspx?lang=th-TH> (accessed on 3 May 2023).
28. Hoehner, P.A. FSK-Based Simultaneous Wireless Information and Power Transfer in Inductively Coupled Resonant Circuits Exploiting Frequency Splitting. *IEEE Access* **2019**, *7*, 40183–40194. [[CrossRef](#)]
29. Adly, I.; Ragai, H.F.; Elhennawy, A.E.; Shehata, K.A. Adaptive packet sizing for OTAP of PSoC based interface board in WSN. In Proceedings of the 2010 International Conference on Microelectronics, Cairo, Egypt, 19–22 December 2010; pp. 148–151. [[CrossRef](#)]
30. Goldsmith, A. *Wireless Communications*; Cambridge University Press: Cambridge, UK, 2005.
31. Yin, X.; Cheng, X. *Propagation Channel Characterization, Parameter Estimation, and Modeling for Wireless Communications*; Wiley: Singapore, 2016.

Disclaimer/Publisher’s Note: The statements, opinions and data contained in all publications are solely those of the individual author(s) and contributor(s) and not of MDPI and/or the editor(s). MDPI and/or the editor(s) disclaim responsibility for any injury to people or property resulting from any ideas, methods, instructions or products referred to in the content.